Identification and estimation of hydrological contributions in a mixed land-use catchment based on a simple biogeochemical and hydro-meteorological dataset

Olivier Grandjouan, Flora Branger, Matthieu Masson, B. Cournoyer, Marina Coquery

Identification and estimation of hydrological contributions in a mixed land-use catchment based on a simple biogeochemical and hydro-meteorological dataset

Olivier Grandjouan[1], Flora Branger[1], Matthieu Masson[1], Benoit Cournoyer[2], Marina Coquery[1]

[1]INRAE, UR Riverly, Centre de Lyon-Villeurbanne, Villeurbanne, France
[2]Univ Lyon, UMR Ecologie Microbienne (LEM), Université Claude Bernard Lyon 1, Marcy L'Etoile, France

Correspondence : ograndjouan@gmail.com ; RiverLy, INRAE, 5 rue de la Doua, Villeurbanne, France, 69625

Abstract

Water pathways and water contamination in mixed land-use catchments are complex to understand. Runoff-generating sources can be numerous and water pathways modified by anthropogenic elements. Monitoring surveys considering geochemical and microbial parameters, are often carried out on such catchment, but are often simple in terms of studied parameters. Nonetheless, they can be helpful to identify the specific signatures of the main runoff-generating sources and estimate their contribution to total runoff at the outlet of mixed land-use catchments. Based on a monthly biogeochemical monitoring program conducted between 2017 and 2019 in the Ratier catchment (19.8 km2) near Lyon (France), a step-by-step approach was developed to : (1) identify the main runoff-generating sources using a perceptual model of the Ratier catchment, (2) identify the respective biogeochemical signatures of each source using this biogeochemical dataset and hydro-meteorological indicators and (3) estimate their contribution to the stream total runoff using an End-Member Mixing Analysis method. We identified three main runoff-generating sources outside of rainy periods : a colluvium aquifer, a fractured gneiss aquifer and a saprolite layer. The monitored geochemical datasets were found divided into three groups matching these sources. Contributions of these sources were estimated based on representative tracer concentrations. Microbial parameters showed a homogeneous agricultural and anthropogenic contamination among the catchment surface water, but also deeper into the fractured gneiss groundwater. This approach showed the potential of using simple monitoring datasets to identify runoffgenerating sources and estimate their contribution to total runoff.

Keywords : biogeochemical signature, microbial parameters, mixing model, monitoring survey, perceptual model, runoff-generating sources

1 Introduction

In 2007, about half of the global population lives in urban areas (Paulet, 2009) and projections from the United Nations predict an increase to over 68% in 2050 (United Nations, 2019). The expansion of urban areas leads to modifications of water natural pathways. Mixed land-use catchments are the first affected by these modifications (Mejía et Moglen, 2010). The land cover diversity in these catchments influences the quantity and quality of stream water. Urban areas can increase flow velocity, decrease water infiltration or cause sewer overflows (Lafont et al., 2006 ; Walsh et al., 2005). Agricultural activities can bring significant amount of pesticides (Giri et Qiu, 2016) or faecal contamination (Marti et al., 2017) to stream water. Impervious surfaces and sewage networks also generate new pathways for pollutants and microbial contaminants transport (Bouchali et al., 2022 ; Navratil et al., 2020 ; Wilson et Weng, 2010). A good understanding of water pathways could help improving water management in these mixed land-use catchments (Jankowfsky et al., 2013).

Many studies have shown the potential of geochemical data to provide insights into water pathways, which could not be inferred by rainfall-runoff dynamics alone (Birkel et Soulsby, 2015). Since the late 1960s, isotope tracer techniques were applied to decompose total runoff between pre-event and event-water (Klaus et McDonnell, 2013). Christophersen et Hooper (1992) introduced the End-Member Mixing Analysis (EMMA) method to identify runoff-generating sources contributing to streamwater and their geochemical concentrations. Runoff-generating sources can be of different kinds : hydrological components, such as surface, subsurface or groundwater (e.g., Ladouche et al., 2001), geomorphological features such as hillslopes (e.g., Burns et al., 2001), specifics land covers (e.g., McElmurry et al., 2014), or point sources like sewer overflow devices (e.g., Lamprea et Ruban, 2011). Specific parameters can be considered as tracers of the runoff-generating sources, with typical concentrations representing the signatures of these sources. They are used to estimate source contributions to streamwater by solving a mixing model using different approaches (e.g., non-negative least square, Bayesian method). To date, the use of conservative tracers within such model is often limited to classical geochemical parameters like stable isotopes, major ions or trace elements (Barthold et al., 2011). Other parameters also showed good potentials for discriminating sources, such as dissolved organic matter (e.g., Boukra et al., 2023 ; McElmurry et al., 2014), organic micropollutants (e.g., Tran et al., 2019), and microbial parameters (e.g., Marti et al., 2017).

However, providing enough data to discriminate sources can be challenging. Most studies identifying runoff-generating sources from stream geochemistry are based on long-term data collected over several years or decades (e.g., Hrachowitz et al., 2009 ; Tetzlaff et al., 2007). According to Aulenbach et al. (2021), such studies are conducted at specific time scales (e.g., hydrological event, monthly sampling) and space scales (e.g., direct source sampling, streamwater sampling), with specific analysis adapted to source identification (e.g., isotopic data). These monitoring can be expensive and complex to set up (Knapp et al., 2020). Alternatively, simple biogeochemical datasets are often produced as part of national monitoring programs involving 1000 of streams in the world to detect global trends in terms of water quality changes (Haag et Westrich, 2002). These data corresponds generally to classical geochemical or microbial parameters, cheap to produce and analysed at a regular frequency (Argent et al., 2007). They are often linked to hydrometeorological data such as discharge and precipitations measures. These datasets are

simpler and they are often open-access. They could bring sufficient data to determinate runoff-generating sources signatures from streamwater concentrations, without requiring additional source sampling. Such method has not been applied so far, to our knowledge. Applying this method, though, requires a correct understanding of the hydrological pathways of a catchment.

Perceptual models are useful additional tools to represent hydrological pathways of a catchment. They are qualitative representations of hydrological dynamics of a catchment, used to illustrate their main components, behaviour and interaction, in visual or textual form (Fenicia et McDonnell, 2022). They are based on hydrologists' personal knowledge and perception (Beven, 1991). Perceptual models are considered as a first step towards the development of a conceptual and/or a physically based hydrological model (Fenicia et al., 2014). Since the 1980s, many studies have used these models to identify runoff-generating sources (e.g., Kendall et al., 2001 ; McGlynn et al., 2002 ; Peters et al., 2003). They can be enriched by visual observations and field data measurements (Beven, 2012 ; McGlynn et al., 2002). Field data can include the use of dye tracing (e.g., Mosley, 1979), trench studies (e.g., McDonnell, 1990), soil moisture, rainfall, groundwater levels (e.g., McMillan et al., 2010 ; McMillan et al., 2011), base flow index (e.g., Gnann et al., 2021), or streamwater geochemical data (e.g., McGlynn et al., 2002 ; Pearce et al., 1986). This paper presents a methodology for the indirect identification and estimation of the runoff-generating sources contribution to the stream total runoff, applicable to a simple biogeochemical and hydrometeorological dataset and based on a perceptual model. The dataset used is from a 3-year monthly monitoring campaign conducted at two stations in the Ratier catchment and its nested subcatchment named, the Mercier (France). A perceptual model of the Ratier catchment was built as a first step from geological, soil and land cover data to identify the main runoff-generating sources. As a second step, the biogeochemical dataset was used to indirectly define the signatures of each source and to select representative tracers. Lastly, the sources contribution to total runoff were estimated using an mixing model, and used to validate the consistency of the runoff-generating sources expected from our perceptual model.

2 Materials and methods

2.1 Study catchment : The Ratier catchment

The Ratier catchment is a subcatchment of the Yzeron basin located west of Lyon, in France. It is part of the Field Observatory in Urban Hydrology (OTHU) and the Critical Zone Observatories : Research and Application, two French national observatories dedicated to long term hydrological monitoring. It covers an area of 19.8 km² and has an altitude ranging between 250 and 780 m.

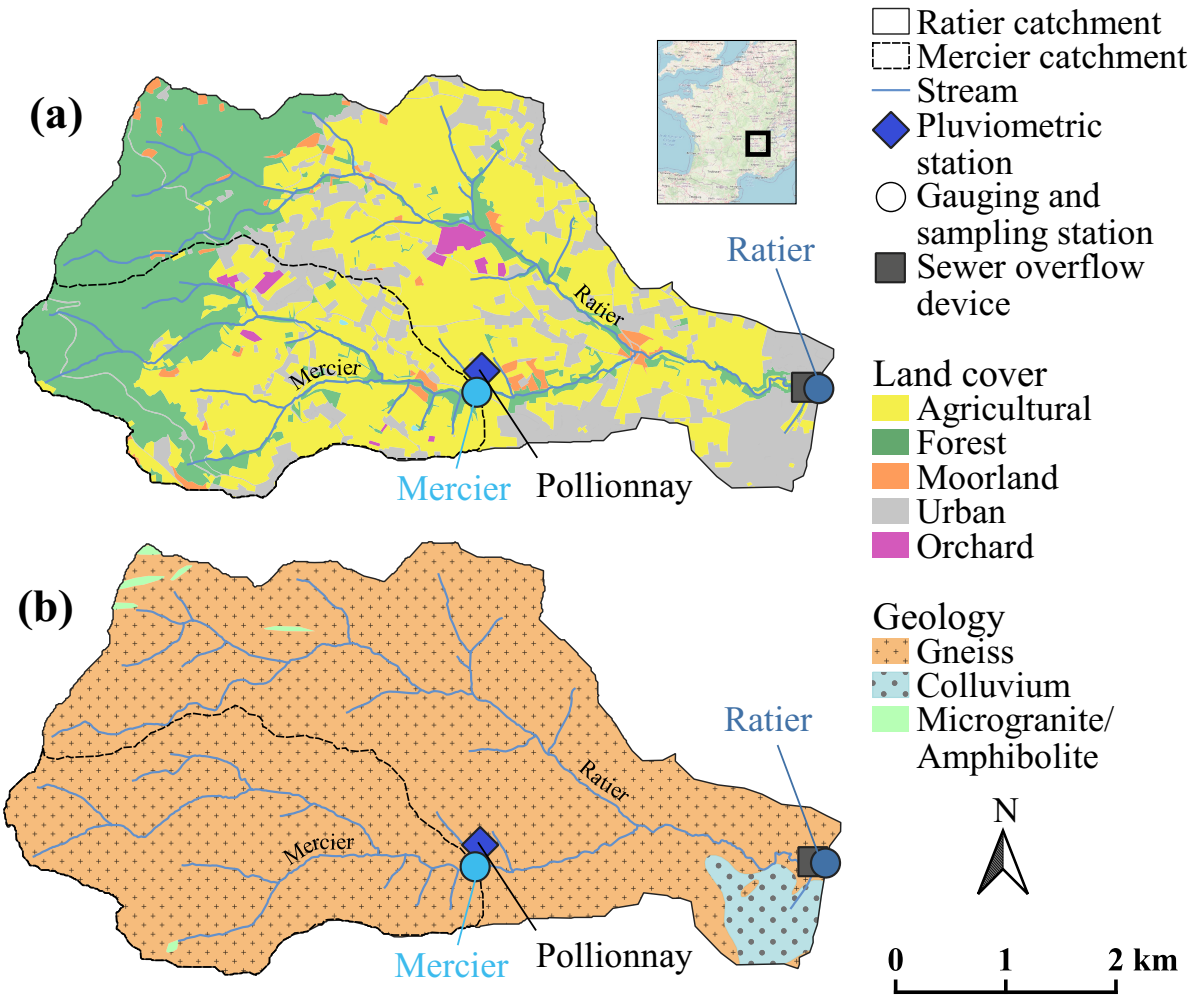

Figure 1 – Maps of the Ratier catchment showing monitoring stations, (a) land cover and (b) geology.

The catchment is characterized by a crystalline geology with gneiss underlying 96% of the total surface (1). The shallow part of the gneiss formation is fractured and gradually changes to a saprolite layer composed of weathered clayous-sandy material and gneiss fragments (Goutaland, 2009). Depth of saprolite varies from less than 1 m in the upper part of the catchment to 10 to 20 m in the valley bottom (Goutaland, 2009). Thin sandy to loamy soils overlay this saprolite layer. As there is no clearly defined delimitation between the saprolite and soil layers (Braud et al., 2011), only the term saprolite will be used in the present study. The fractured part of the crystalline bedrock provides low perennial

groundwater storage (Delfour et al., 1989). The saprolite layer can have significant but localized and heterogeneous water storage capacities at the valley bottom or in local discontinuities (Braud et al., 2011). Downstream of the catchment, the eastern part is covered by colluvium deposits mixing clayous sands, bedrocks fragments (e.g., granite, gneiss), siliceous pebbles and a clayous-ferroginous matrix (David et al., 1979) (Figure 1). Thin calcareous soils cover the colluvium deposits. The colluvium formation holds a local aquifer.

The Ratier catchment is a typical mixed land-use catchment with heterogeneous land cover that includes urban areas (15% by catchment area), agricultural areas (44%), and forest (42%) (Branger et al., 2013). In urban areas, wastewater and rainwater are managed by a combined sewer network and transferred outside the limits of the catchment ; however, they can be released in streams through the use of combined sewer overflow devices (Figure 1).

The Mercier stream is a tributary of the Ratier stream with a catchment of 7.8 km^2. It is less urbanized than the Ratier catchment (5% of total surface) and has a higher proportion of agricultural land cover (52%). Forests represent 42% of the total area. The Mercier stream is often dry in summer and early autumn (June to October). The catchment climate is temperate with Mediterranean and continental influences (Gnouma, 2006). The mean annual precipitation is 820 mm and the mean annual minimum and maximum temperatures are 8.6 and 17.5°C from 1991 to 2020 (Météo-France, 2023).

2.2 Field data

Hydro-meteorological data

Two nested gauging stations are located at the outlets of the Ratier and Mercier catchment (Figure 1) ; stream water levels and water temperature are measured since 2010 and 1997, respectively. Discharges are calculated at both stations from stream water levels using rating curves. The pluviometric station of Pollionnay is a weighing device recording rainfall amounts and air temperature (Figure 1). Discharge, rain and temperature data are available on the Hydrology Observatory Data Base (BDOH) (Lagouy et al., 2015). In this study, we used mean daily discharge from the Mercier and Ratier gauging stations ; and mean daily rainfall from the Pollionnay pluviometric station. Daily reference evapotranspiration data was calculated from the SAFRAN reanalysis, a mesoscale analysis system for atmospheric surface variables, developed by Meteo France over the whole French territory on 8×8 km2 grid cells (Le Moigne et al., 2020). We used cell n°6331 at a daily timestep.

Sample collection

Monthly monitoring campaigns were conducted from March 2017 to December 2019 at the outlets of the Mercier and Ratier streams (Figures 1 and 2). A total of 24 samples were taken at the Mercier gauging station and 26 samples at the Ratier gauging station. These samples were collected manually in sampling bottles positioned below the water

surface (Table 1). No sampling campaign was done during raining events. These campaigns are similar to these of the French national geochemical monitoring program, which consist of subsurface grab sampling at a regular frequency, whatever the meteorological or hydrological conditions (Lepot et Marescaux, 2022).

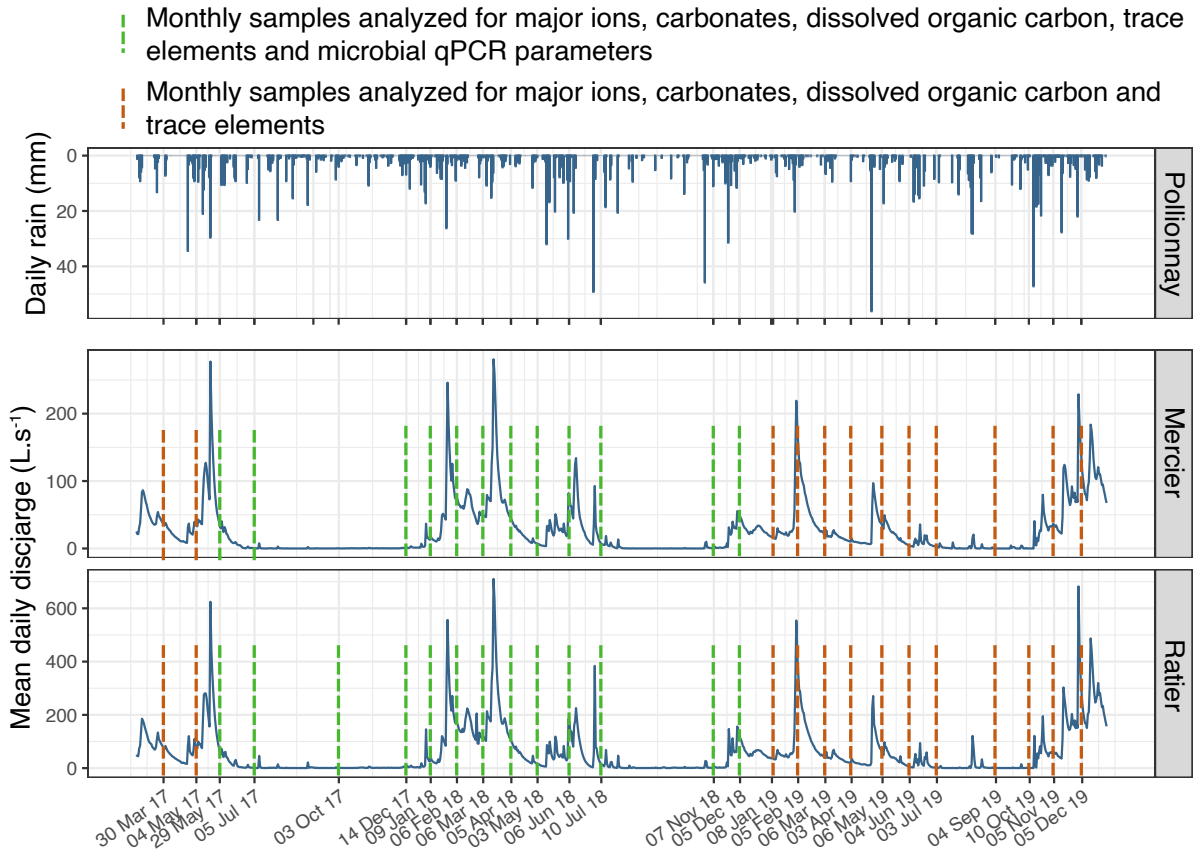

Figure 2 – Daily precipitation at the Pollionnay pluviometric station and mean daily discharge at the Mercier and Ratier gauging stations from 2017 to 2019. Dashed lines correspond to the monthly manual samples and colours to the corresponding analysis.

Samples were filtered at 0.45 µm and analysed for a set of 35 biogeochemical parameters, including geochemical and microbial parameters. Geochemical parameters included 8 major ions, carbonates, dissolved silica, dissolved organic carbon and 20 trace elements (Table 1). Four microbial DNA targets were tracked using a quantitative Polymerase Chain Reaction method (qPCR) (Table 1). These qPCR assays were performed on DNA extracts from 13 samples collected at the Ratier station and 12 at the Mercier station collected between May 2017 and December 2018 (Figure 2). DNA extracts were performed as indicated in Pozzi et al. (2024). Table 1 shows a complete list of the measured biogeochemical parameters and their respective methods. Major ions were analysed by ion chromatography, as their ionic forms are the main form observed in the dissolved phase of surface water, unlike trace elements, which were analysed using inductively coupled mass spectrometry (ICP-TQ-MS). The absence of contamination was systematically confirmed by the analysis of blanks. qPCR assays for a human (HF183 DNA target) and ruminant (rum-2-bac DNA target) faecal emitters were done as described in Marti et al. (2017). The clinical class 1 integron PCR assay was performed according to Gassama Sow et al. (2010), and allowed a tracking of an integrase coding sequence specifically harboured by integron 1 (genetic shuttles) encoding antibiotic resistances. The qPCR assay for tracking Pseudomonas aeruginosa was performed according to Colinon et al. (2013).

Table 1 – Measured biogeochemical parameters, respective analytical method and sampling material. PEHD = Polyethylene high-density ; DOC = Dissolved Organic Carbon

Chemical familly or name	Biogeochemical parameter	Method	Sampling material
Major cations	Ca^{2+}, K^{+}, Mg^{2+}, Na^{+}	Ionic chromatography NF EN ISO 14911 (AFNOR, 1999)	
Major anions	Cl^{-}, NO_3^{-}, SO_4^{2-}, PO_4^{3-}	Ionic chromatography NF EN ISO 10304-1 (AFNOR, 2009)	
Silica	SiO_2	Colorimetry	
Carbonates	HCO_3^{-}	Potentiometric titration NF EN ISO 9963-1 (AFNOR, 1996)	1 L PEHD plastic bottle
Trace elements	Al, As, B, Ba, Co, Cr, Cu, Fe, Li, Mn, Mo, Ni, Pb, Rb, Sr, Ti, U, V, Zn	ICP-MS NF EN ISO 17294.2 (AFNOR, 2016)	
Dissolved Organic Carbon	DOC	Catalytic combustion with IR measurement	250 mL glass bottle
Microbial DNA targets	human Bacteroides marker HF183, ruminant Bacteroides marker rum-2-bac, Pseudomonas aeruginosa, Clinical class 1 integron	qPCR assay	2 L PEHD plastic bottle

2.3 Runoff-generating sources modelling

Assumptions on the main runoff-generating sources : Perceptual model

The identification of the runoff-generating sources was based on a perceptual model of the Ratier catchment hydrological behaviour. The Figure 3 illustrates the model we built on the basis of the framework proposed by Wagener et al. (2007) who described the dominant hydrological functions that can regulate a catchment. Meteoric waters are intercepted by vegetation and impervious areas. Surface runoff from the road and other impervious areas is transferred quickly to the sewer network or to the closest stream. Combined sewer overflows can release sewer network waters during heavy rain events. In rural and forested areas, rainwater infiltrates through the saprolite layer. When the catchment is dry, the saprolite layer is not saturated, and water can infiltrated further down to fill the upper part of the gneiss formation, which is highly fractured and permeable. This permeability, albeit spatially variable, allows the water to flow downhill and to join the streamwater at the valley bottom. This fractured gneiss groundwater is thus considered as the main contribution to the stream when the catchment is dry. In contrast, when the catchment is wet, the saprolite layer becomes saturated in water, resulting in the generation of a saprolite water flow and acting as an additional contribution to stream flow.

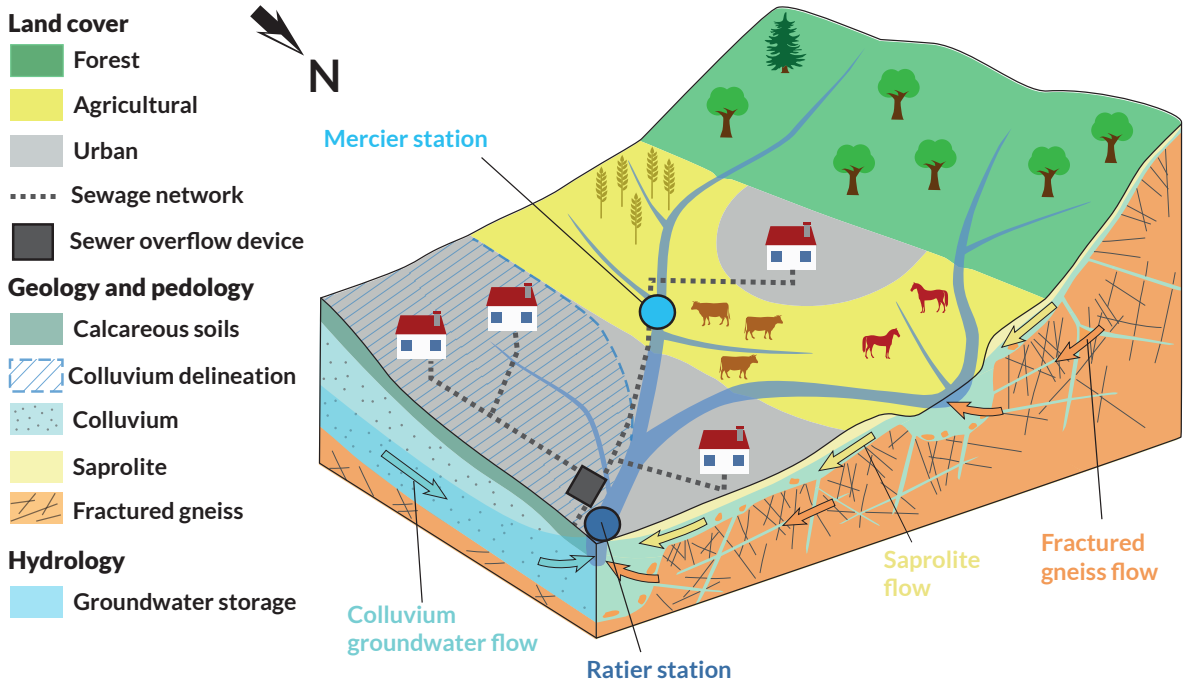

Figure 3 – Perceptual hydrological model of the Ratier catchment.

We made the following assumptions on biogeochemical signatures based on this perceptual model. At low flow, the fractured gneiss groundwater forms the unique contribution to the upper streams (the Mercier stream and the upper Ratier stream before the confluence) ; the biogeochemical signature of the upper streams is expected to be representative of the fractured gneiss groundwater. At high flow, the saprolite water flowing through the saprolite layer act as the major contributor to the stream water ; the biogeochemical signature of the upper streams is expected to be representative of the saprolite water. Perennial groundwater storage is found in the eastern colluvium deposits that continuously supplies the Ratier stream, downstream of the catchment. At the outlet of the Ratier catchment, both the fractured gneiss groundwater and colluvium groundwater are contributing to the total runoff. However, when the upper streams are dry, only the colluvium aquifer supplies the Ratier stream ; so the stream water composition is expected to be representative of the colluvium aquifer groundwater. In this study, as no sampling campaign was done during raining events, direct surface runoff could not be considered.

Assessment of biogeochemical signatures for the main runoff-generating sources

Hydro-meteorological indicators were calculated to characterize flow conditions according to hydrological and meteorological variables. Previous Day Discharge (PDD) is the mean daily discharge the day before sampling. Five-day Antecedent Rain (AR5) represents rainfall accumulation over the five past days and reflects soil wetness. They were calculated for each sampling date. The resulting indicator values were then classified into three categories : low, intermediate and high, according to an equal-size discretization based on quantiles. Each sample was associated with its corresponding hydro-meteorological indicator class. Low flow conditions can be characterized by low PDD and low AR5 whereas high flow conditions correspond to high PDD and high AR5.

Major ions, carbonates, dissolved silica, dissolved organic carbon and trace elements were used together with the hydro-meteorological indicators to distinguish geochemical signatures among fractured gneiss groundwater, colluvium groundwater and saprolite waters. We excluded from our working database parameters measured too close to their limit of quantification (parameters PO_3^- and Cd ; see Table S1S). First, Spearman correlation and hierarchical cluster analysis (HCA) were applied to group geochemical parameters with similar behaviour. The optimal number of clusters in the HCA was found by using the elbow method (Thorndike, 1953), which minimize the total intra-cluster variation. Positively correlated geochemical parameters could imply a similar runoff-generating origin. We also applied a Spearman correlation between the geochemical parameters and the three hydro-meteorological indicators to highlight significant relations between concentration and catchment hydro-meteorological conditions. Second, a Kruskal-Wallis-Dunn non-parametric test was applied to identify significant difference in parameters concentration (i) between low PDD samples and remaining samples, (ii) between high PDD samples and remaining samples and (iii) between high AR5 samples and remaining samples. For the Spearman correlation analysis and Kruskal-Wallis-Dunn non-parametric test, we used the R software (R Core Team, 2020) and Factoshiny Package (Vaissie et al., 2021).

The microbial dataset was used to distinguish between agricultural and urban signatures for the saprolite water. As the number of samples for microbial parameters was too low for applying KruskalWallis between the three classes of indicators (low, intermediate, high), we scrutinized relations between concentrations and the hydrometeorological indicators through a Spearman correlation analysis. A Kruskal-Wallis analytical test was applied to seek for significant differences between the two sampling stations. As the downstream part of the catchment is more urbanized and a sewer overflow device is located just upstream the Ratier station, higher contribution of anthropogenic contamination was expected at the Ratier station.

Estimation of runoff-generating sources contributions to total runoff

We applied a mixing model method to estimate runoff-generating sources contributions to total runoff. This method is used to decompose a mixed volume of water (here the stream) into several endmembers contributions (here the identified runoff-generating sources). The end-member concentrations were inferred from streamwater concentrations. Such indirect way is part of an EMMA approach. Two end-members were considered at the Mercier station corresponding to the fractured gneiss groundwater and the saprolite water flow. The colluvium aquifer was considered as a third endmember at the Ratier station. The mixing model method uses tracers, which are geochemical parameters selected to characterize each endmembers and estimate their contributions. The resolution of the mixing model equations requires at least n-1 tracers for n end-members. We choose to select one tracer per source, considering that the selection of larger number of tracers has more chance to bring false conclusions about the estimated contributions (Barthold et al., 2011). Tracers had to be conservative, additive and representative of each endmember. Conservativeness of tracers was evaluated using Poubraix diagram to evaluate their chance to be modified according to the expected pH and redox of the stream. Tracers were then selected among the representative geochemical parameters for each runoffgenerating source. Selection was based on results from the Kruskal-Wallis-Dunn, literature and knowledge of the geochemistry of the area to assess its representativeness. We chose

to represent each end-member by the maximum concentration measured for its representative tracer as we expect extreme concentrations to be more representative of sources signatures. We expected the representative tracer of a given end-member to be present at low concentration in the two other end-members, and therefore assigned the minimum concentrations observed to these end-members. The choice of the final combination of tracer was confirmed with mixing diagrams, which are plots showing the repartition of end-members and streamwater samples concentrations. A complete EMMA approach would consist to apply a Principal Component Analysis to visualize the mixing diagram. As we chose to select unique concentrations for each source and tracer, we did not follow the full EMMA approach and represent mixing diagrams by 2-D plots for each pair of tracers. The chosen tracers and concentrations can be considered representative of each end-member if the general shape includes all the samples concentrations for all mixing diagrams. The mass of a tracer measured at the outlet is considered equal to the sum of tracer coming from each end-member (Pinder et Jones, 1969). The system can be resolved in a mixing model as follows :

$$\sum_{i}^{n} Q_i(t) \times C_{k,i} = Q_{\text{tot}}\,(t) \times C_k(t) \tag{1}$$

where n is the number of end-members, Q_i the discharge from endmember i and Q_{tot} the total discharge at the outlet, $C_{k,i}$ the concentration of tracer k in end-member i and C_k is the concentration of tracer k at the outlet. We used *nnls* Package in *R* to solve the mixing model system through a non-negative least square regression (Mullen et van Stokkum, 2012).

3 Results

3.1 Assessment of the biogeochemical signatures for the main runoff-generating sources

Clustering of geochemical parameters

Concentrations of the geochemical parameters measured at the Mercier and Ratier stations are reported in Table S1S. Figure 4 shows the results of the hierarchical clustering analysis (for geochemical parameters only) and Spearman correlation for all data from both station (geochemical parameters and hydro-meteorological indicators). The Elbow method gave an optimal number of four clusters for the 29 geochemical parameters considered. Cluster 1 shows the most positively correlated group of parameters, composed of the major ions Ca^{2+}, Mg^{2+}, HCO_3^- and SO_4^{2-}, and the trace elements Sr, Ba, Li, U and Mo. Parameters Ca^{2+}, Mg^{2+}, Sr and Ba have the highest similarity with correlation factors >0.9. The alkaline earth elements (Ca, Mg, Sr and Ba) are common components of geological formations ; as they are reactive, their ionic forms are often found in groundwater (Appelo et Postma, 2004). They have shared physical and chemical properties due to their similar electronic structures, consisting of a pair of electrons, which can explain their high correlation factors. The parameters SO_4^{2-}, Li, U and Mo can have both natural and anthropogenic origins, but they are often geology-related (Deverel et al., 2011). The negative correlations between Li or HCO_3^- and the PDD indicator (r = -0476. and -0.532, respectively) indicates that concentrations for these parameters tend to be higher at low flow. This could suggest that Li, HCO_3^- and their positively correlated parameters from cluster 1 could be tracers of groundwater contribution. Four parameters of cluster 2 (Cl^-, Na^+, K^+ and Rb) are positively correlated with parameters of cluster 1 ; and two are also negatively correlated with the PDD indicator (Na^+ and Rb). Thus, cluster 2 may also include tracers of a groundwater contribution. Cluster 3 contains several parameters known to be influenced by redox reactions (Fe, Mn, As, V) and may not represent a specific runoff-generating source. Finally, for cluster 4, positive correlations are shown between Al, Cr, DOC, Ni, NO_3^-, Cu, Ti and the indicators PDD and AR5. Parameters Al and Cr showed the strongest correlation with PDD, with respective correlation coefficient of 0.822, 0.829. These correlations suggest a shared origin for these parameters, linked to high flows and wet conditions. Concentrations of these geochemical parameters tend to be higher at high flow and could be tracers of a shallower contribution flowing through the saprolite layer. The negative correlation between Al and Cr with several elements of clusters 1 and 2 confirms the opposition between two geochemical signatures matching a global groundwater contribution and a saprolite water contribution.

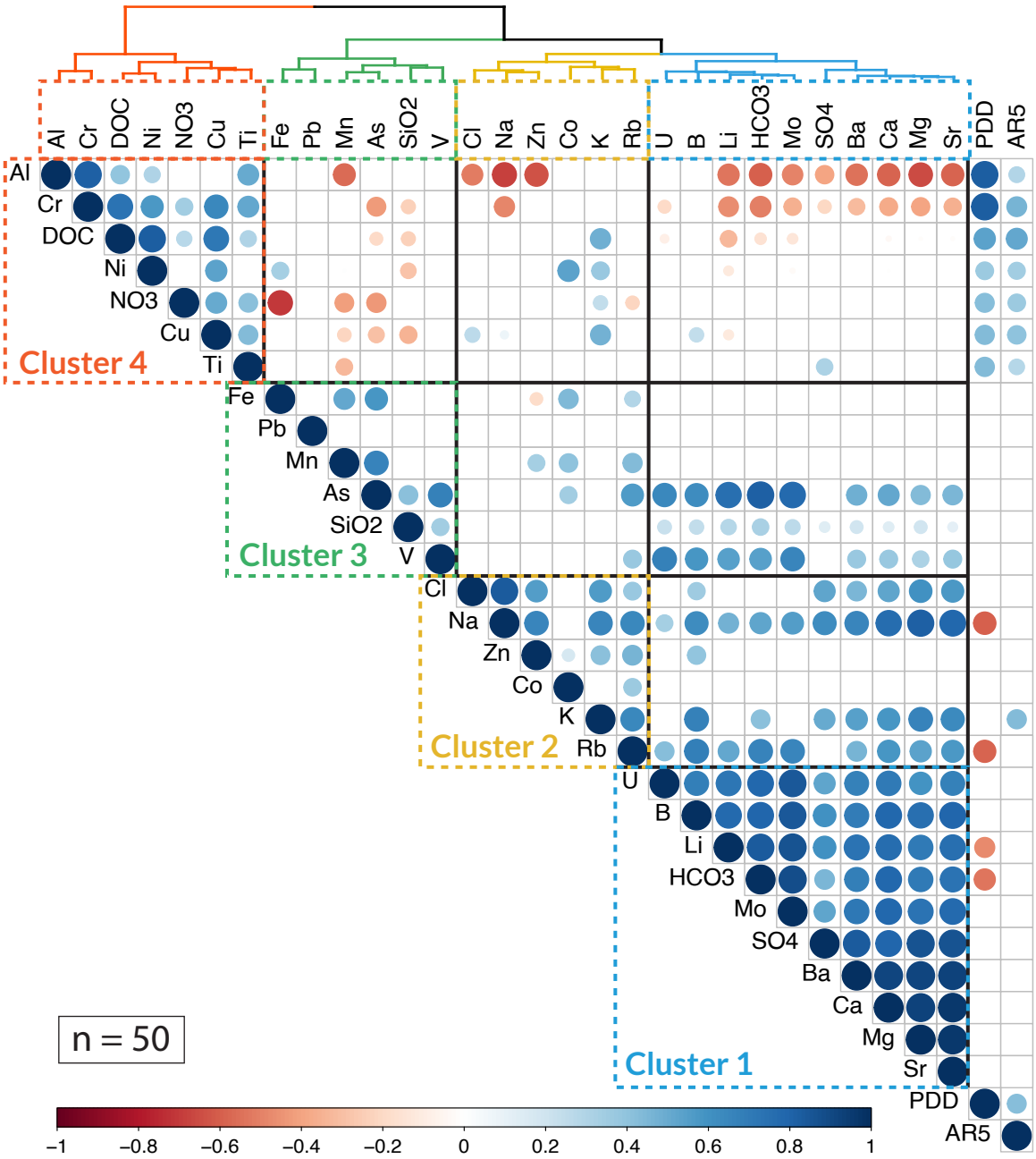

Figure 4 – Results of the hierarchical clustering analysis (HCA) for geochemical parameters only and Spearman correlation for geochemical parameters and hydro-chemical indicators at the Mercier and Ratier stations. Only significant correlation factors ($p < 0.05$) are shown. Dashed rectangles illustrate the 4 clusters obtained from the HCA. PDD : Previous Day Discharge ; AR5 : 5-day Antecedent Rain.

Linking geochemical parameters with runoffgenerating sources

Results of the Kruskal-Wallis-Dunn test between groups of concentrations are shown in Table 2 for the 23 geochemical parameters considered (Figure 4). At the Mercier station, B, Li, HCO_3^-, Ba, Ca^{2+}, Mg^{2+}, Sr, Zn, Co, K and Rb showed significantly higher concentrations for the low PDD samples. According to the assumptions of the perceptual model, the concentrations of these 11 geochemical parameters measured at low flow in the upper streams (i.e., at the Mercier Station) are the most representative of the fractured gneiss groundwater.

In contrast, Al and Cr showed significantly higher concentrations for high PDD samples at both stations. Moreover, Al and Cr were significantly higher for high AR5 at the Mercier station, which may favour the transport of these compounds present at the surface or within the saprolite layer. Parameter Al was well quantified, as the minimum measured value was at least twice the limit of quantification. As Al showed the lowest p-value for the Kruskal-Wallis-Dunn comparison between high PDD samples and remaining samples, we considered this parameter as the most representative geochemical parameter of the saprolite water flow.

Table 2 – p-value of the Kruskal-Wallis-Dunn test comparing the differences in concentrations between i) samples taken at low Previous Day Discharge and other samples, ii) samples taken at high Previous Day Discharge and other samples and, iii) samples taken at high 5-day Antecedent Rain and other samples. Blues cells indicate significantly lower concentrations and red cells significantly higher concentrations. PDD : Previous Day Discharge ; AR5 : 5-day Antecedent Rain.

		Mercier			Ratier		
	Par.	**i) Low PDD samples VS other samples**	**ii) High PDD samples VS other samples (n = 12)**	**iii) High AR5 Samples VS other samples (n = 10)**	**i) Low PDD samples VS other samples (n = 6)**	**ii) High PDD samples VS other samples (n =12)**	**iii) High AR5 samples VS other samples (n =11)**
Cluster 1	U	0.64	0.49	0.25	**0.001**	**0.001**	0.24
	B	**0.02**	**0.05**	0.51	0.06	**0.001**	0.54
	Li	**0.002**	**0.001**	0.52	**<0.001**	**<0.001**	0.14
	HCO_3^-	**0.005**	**0.04**	0.58	**<0.001**	**<0.001**	0.13
	Mo	0.1	**0.03**	0.52	**<0.001**	**<0.001**	0.19
	SO_4^{2-}	0.94	0.91	**0.01**	**0.01**	**0.002**	0.76
	Ba	**0.005**	**0.04**	0.47	**0.002**	**0.001**	0.98
	Ca^{2+}	**0.01**	**0.03**	0.37	**0.001**	**<0.001**	0.64
	Mg^{2+}	**0.02**	**0.04**	0.34	**0.004**	**<0.001**	0.94
	Sr	**0.02**	**0.04**	0.31	**0.001**	**<0.001**	0.68
Cluster 2	Cl-	0.73	**0.05**	0.25	0.18	**0.02**	0.54
	Na^+	0.06	**0.03**	0.4	**0.005**	**0.001**	0.78
	Zn	**0.002**	**0.02**	0.88	**0.03**	**0.01**	0.68
	Co	**0.05**	0.07	0.71	0.43	0.76	0.68
	K^+	**0.05**	0.19	0.15	0.93	0.24	0.12
	Rb	**0.008**	**0.03**	0.62	**0.03**	**0.002**	0.68
Cluster 4	Al	**0.01**	**<0.001**	**0.08**	**<0.001**	**<0.001**	0.12
	Cr	0.35	**0.007**	**0.002**	**0.001**	**<0.001**	0.08
	DOC	0.23	0.27	**0.01**	**0.001**	**0.004**	**0.04**
	Ni	**0.02**	0.69	0.43	**0.002**	**0.003**	0.11
	NO_3^-	**0.02**	0.07	**0.01**	0.76	0.84	0.11
	Cu	0.54	0.69	**0.005**	**0.03**	0.16	0.11
	Ti	0.46	**0.05**	**0.04**	**0.08**	0.22	**0.04**

Two groundwater contributions are expected at the Ratier station : the fractured gneiss groundwater and the colluvium groundwater. According to the Kruskal-Wallis-Dunn test, several parameters are representative of both groundwater contributions : Li, HCO_3^-, Ba, Ca^{2+}, Mg^{2+}, Sr, Zn and Rb (Table 2). It is thus necessary to clarify the geochemical signature of these contributions. Considering only samples collected at low PDD, which are the most representative of groundwater, we applied Kruskal-Wallis-Dunn tests to compare groundwater concentrations between the upstream Mercier station and the downstream Ratier station for these specific parameters. Table 3 shows the p-value resulting from this test. Parameters Li, HCO_3^-, Ba, Ca^{2+}, Mg^{2+} and Sr showed significantly higher concentrations at low flow for the Ratier samples, which can be attributed to the colluvium aquifer. Parameter Rb had similar concentrations at both stations, so we assume that the colluvium aquifer did not provide significant inputs to the stream for these elements. Zn concentrations were significantly higher at the Mercier station. We identified parame ters Li, HCO_3^-, Ba, Ca^{2+}, Mg^{2+}, Sr, U, Mo, SO 2- and Na^+ as tracers of the colluvium groundwater, and parameters Zn, Rb, B, Co and K^+ as tracers of the fractured gneiss groundwater (Tables 2 and 3).

Table 3 – p-value of the Kruskal-Wallis-Dunn test comparing the differences in concentrations between the Mercier and the Ratier samples considering only samples collected at low Previous Day Discharge and parameters showing significantly higher concentration at low Previous Day Discharge at both stations.

Chemical parameter	**Mercier samples VS Ratier samples**	**Station with higher concentrations**
Li	**0.01**	Ratier
HCO_3^-	**0.01**	Ratier
Ba	**0.01**	Ratier
Ca^{2+}	**0.01**	Ratier
Mg^{2+}	**0.01**	Ratier
Sr	**0.01**	Ratier
Zn	**0.01**	Mercier
Rb	0.39	-

Table 4 shows median and range of concentration of the identified tracers for the three runoff-generating sources. We selected concentrations measured at low PDD at the Mercier station as representative of the fractured gneiss groundwater, and concentrations measured at low PDD at the Ratier station as representative of the colluvium groundwater. We considered the concentrations measured at high flow at the Mercier station as representative of the saprolite water. Parameter Li showed particularly higher concentration (x10) at the Ratier station compared to the Mercier station. Concentration of Zn was particularly higher (x7) at the Mercier station compared to the Ratier station.

Table 4 – Concentrations of the parameters representative of the identified runoff-generating sources. Coloured and bolded chemical parameters indicate the most representative tracers of each source. PDD : previous day discharge ; AR5 : 5-day antecedent rain.

Runoff-generating source	**Fractured gneiss groundwater**			**Colluvium groundwater**			**Saprolite water**		
Corresponding group of samples	**Low PDD at the Mercier station**			**Low PDD at the Ratier station**			**High PDD at the Mercier station**		
Chemical parameter	**Min.**	**Median**	**Max.**	**Min.**	**Median**	**Max.**	**Min.**	**Median**	**Max.**
Zn ($\mu g.L^{-1}$)	**14.6**	**17.2**	**23.8**	1.6	2.4	4.52	0.7	1.4	2
Rb ($\mu g.L^{-1}$)	**1.17**	**1.71**	**2.37**	1.22	1.42	1.63	0.82	0.97	1.53
B ($\mu g.L^{-1}$)	**15.1**	**17.6**	**39.1**	16.1	25.4	26.8	7.8	12.5	20.8
Co ($\mu g.L^{-1}$)	**0.16**	**0.54**	**1.35**	0.07	0.19	0.27	0.12	0.18	0.27
K^+ ($mg.L^{-1}$)	**3**	**4.2**	**4.7**	2.8	3.4	4.4	1.4	3.2	4.3
Li ($\mu g.L^{-1}$)	0.91	1.26	1.56	**4.69**	**13.6**	**20.6**	0.5	0.62	0.85
HCO_3^- ($mg.L^{-1}$)	65	90	119	**134**	**165**	**196**	42	51	83
Ba ($\mu g.L^{-1}$)	22.5	26.2	32.4	**33**	**39.5**	**46.2**	11.3	19.2	23.2
Ca^{2+} ($mg.L^{-1}$)	26.4	33.9	45.1	**46.6**	**57.2**	**66.9**	14	23.9	29.6
Mg^{2+} ($mg.L^{-1}$)	4.3	5.1	5.4	**5.7**	**7.5**	**8.4**	2.9	4	4.8
Sr ($\mu g.L^{-1}$)	93.7	113	137	**151**	**188**	**210**	54.2	85.4	105
U ($\mu g.L^{-1}$)	0.09	0.16	0.27	**0.42**	**0.92**	**1.61**	0.12	0.16	0.41
Mo ($\mu g.L^{-1}$)	0.17	0.22	0.25	**0.72**	**0.97**	**1.42**	0.12	0.14	0.36
SO_4^{2-} ($mg.L^{-1}$)	12.5	19.7	50.2	**29.3**	**42.6**	**57.7**	13	17.9	28.6
Na- ($mg.L^{-1}$)	21.4	24.55	50.8	**25.4**	**26.95**	**33.1**	16.4	20.3	24.9
Al ($\mu g.L^{-1}$)	4.3	9.1	14.7	6.4	7.8	8.9	**18.5**	**34.7**	**75.3**
Cr ($\mu g.L^{-1}$)	0.12	0.13	0.18	0.06	0.08	0.1	**0.13**	**0.17**	**0.26**
DOC ($mg.L^{-1}$)	6.8	7.7	8.6	2.8	4	5.9	**5.5**	**7.6**	**10**
Ni ($\mu g.L^{-1}$)	0.79	1.29	1.45	0.26	0.62	0.92	**0.65**	**0.91**	**1.18**
NO_3^- ($mg.L^{-1}$)	1	1.8	5.6	4.4	7.6	12.1	**2.6**	**6.8**	**24.2**
Cu ($\mu g.L^{-1}$)	0.65	1.92	5	1.07	1.87	2.05	**1.37**	**2.42**	**3**
Ti ($\mu g.L^{-1}$)	0.27	1.07	2.52	0.26	1.06	2.76	**0.52**	**1.78**	**2.95**

Distinction between rural and urban contribution in saprolite water

Microbial parameters monitored through qPCR assays were used to track human and ruminant faecal contaminations over the catchment and investigate the transfer of these markers into the fractured gneiss (Table S2S and Figure 5). Similar counts of rum-2-bac were observed at the Ratier and Mercier sampling stations. However, a lower urban impact was expected for the Mercier subcatchment due to the absence of sewer overflow device and a lower urban surface area. Nevertheless, high numbers of HF183 markers were observed at both the Mercier and Ratier river stations. Occurrences of these HF183 faecal markers were even detected at low PDD and low AR5. These results suggest that this marker can disseminate with the saprolite waters but also with groundwater. Detection of HF183 indicates significant human faecal contaminations in the Mercier catchment probably related to sewer system leakages or the use of septic tanks in certain parts of the catchment. These human and ruminant faecal contaminations were associated with significant counts of class 1 clinical integrons. The Mercier and Ratier stations could be differentiated by their qPCR counts in *ecfX P. aeruginosa* gene copies. Fewer occurrences (n = 14) of *P. aeruginosa* DNAs were observed in the Ratier stream (n = 2 *ecfX* positive samples) than the Mercier one (n = 6 *ecfX* positive samples), indicating a tropism or more sustained emissions of *P. aeruginosa* in the most rural parts of the catchment (Figure 5). The perceptual model was modified to take in account a significant human faecal contamination of the headwaters of both streams.

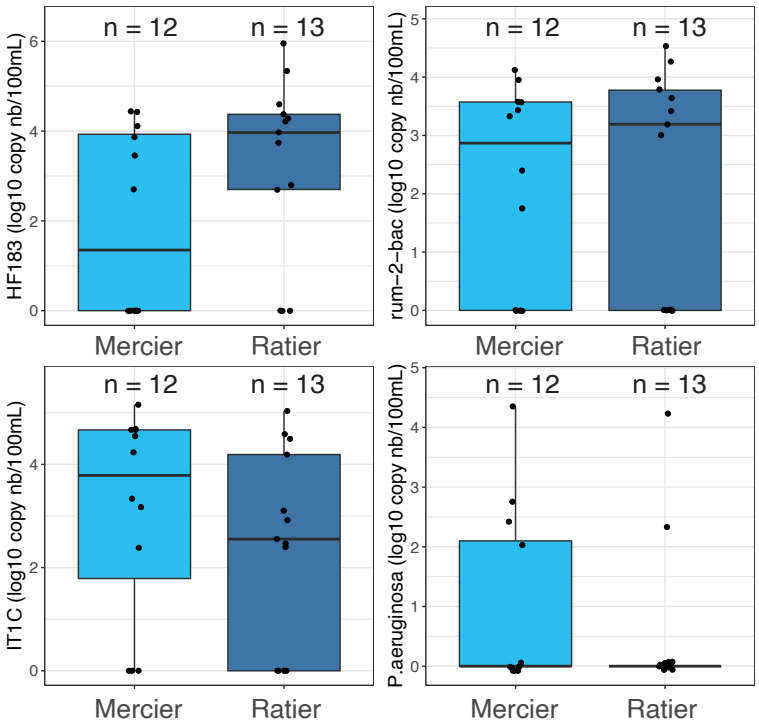

Figure 5 – Concentration of microbial parameters at the Mercier and Ratier stations. n values represent number of values selected. IT1C : Class 1 clinical integron.

3.2 Decomposition of total runoff at the catchment outlet

Choice of tracers and concentrations in endmembers

From the tracers of the fractured gneiss groundwater (Zn, Rb, B, Co and K^+), we chose Zn to represent this end-member. Indeed, Zn concentration at low PDD was about an order of magnitude higher at the Mercier station than at the Ratier station, and the minimum measured concentration was five times higher than limit of quantification (Table 4). The minimum Zn values were also at least five times higher than blank analysis. Li was chosen to represent the colluvium aquifer, as its concentration was particularly high compared to the fractured gneiss groundwater (Table 4). Finally, Al was chosen to represent the saprolite water flow, as it is one of the most correlated parameter with PDD and is concentrations were significantly higher than limit of quantification. Figure 6 shows mixing diagrams of the repartition of samples concentrations for the three selected tracers, according to the class of PDD at both stations. The chosen concentrations seem to be representative of each end-member as the general shape includes all the samples concentrations for the three mixing diagrams.

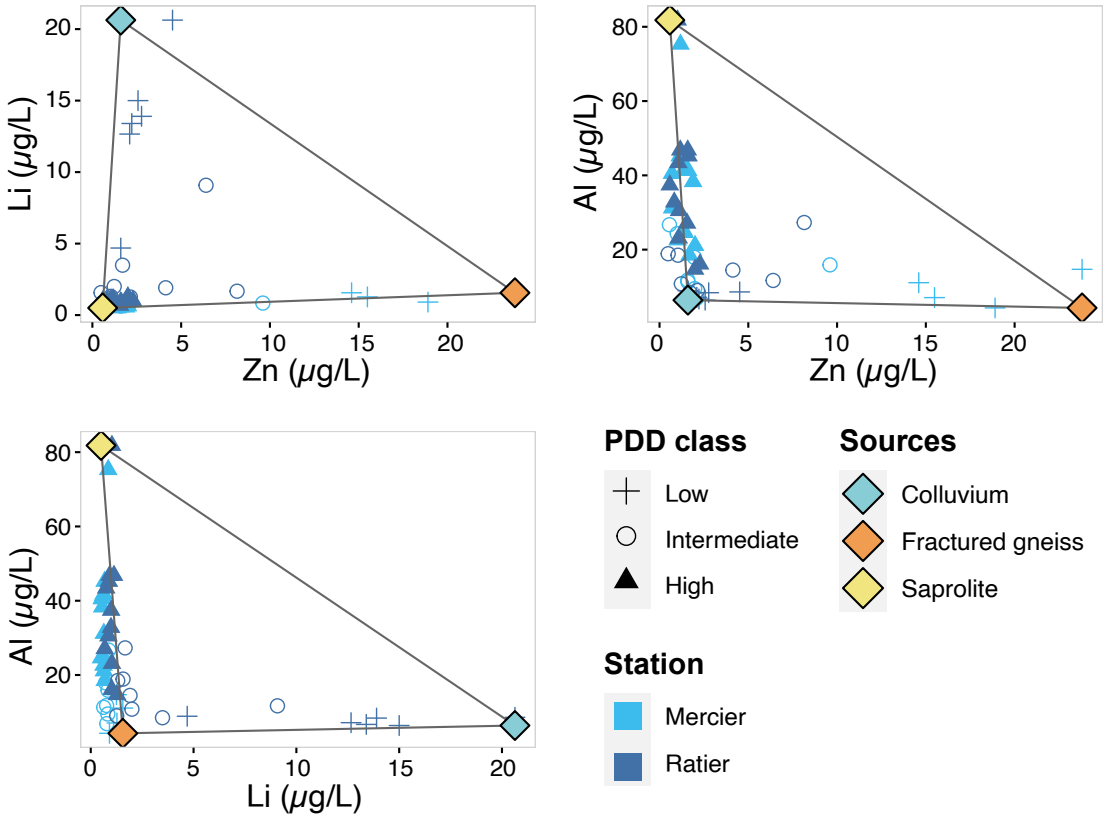

Figure 6 – Mixing diagrams showing samples and end-members concentrations of Zn, Li and Al at the Mercier and Ratier stations. PDD : Previous Day Discharge.

Estimation of source contributions resolving a mixing model

Figure 7 illustrates the results of model estimations of the contribution of the two end-members to total runoff at the Mercier station, and of the three end-members to total runoff at the Ratier station. The fractured gneiss groundwater contribution is prevalent at the Mercier station, particularly at low flow (typically from September to December). The fractured gneiss showing low and discontinuous groundwater storage capacity, this contribution at low flow may explain the disconnection of the upstream part of the catchment in summer. At low flow, the colluvium aquifer tends to be the major contributor to total runoff at the Ratier station. The seasonality is marked by higher groundwater contribution (both colluvium and fractured gneiss) between June and November, and higher saprolite water contribution between February and June.

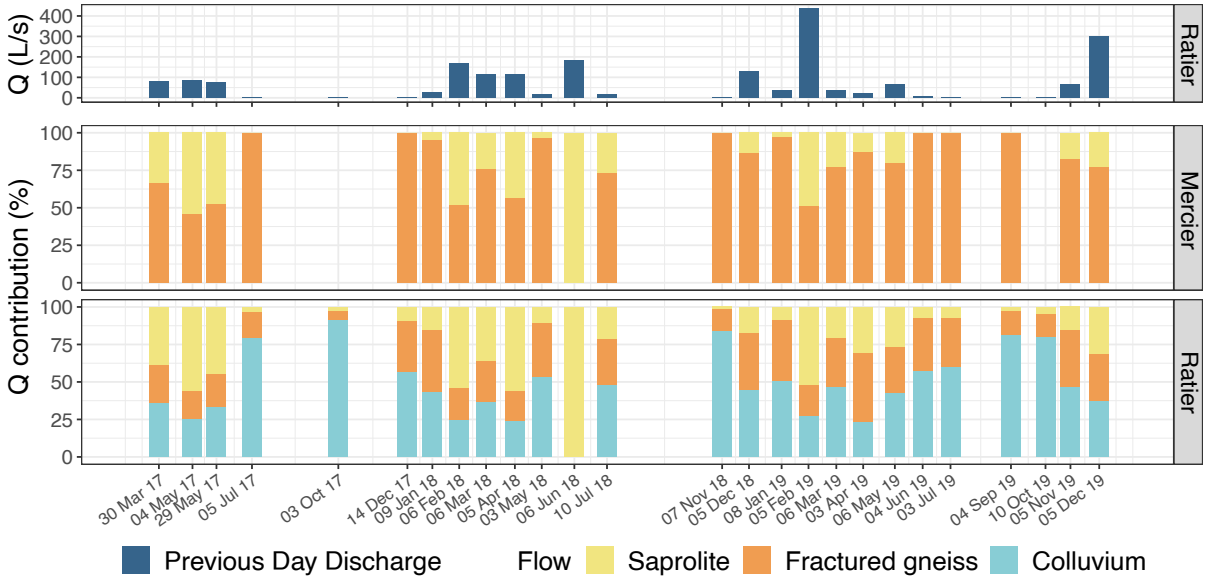

Figure 7 – Mixing diagrams showing samples and end-members concentrations of Zn, Li and Al at the Mercier and Ratier stations. PDD : Previous Day Discharge.

The variations of the estimated contributions of end-members for each sample and PDD are shown in Figure 8. The fractured gneiss groundwater contribution has a significant negative correlation with PDD at the Mercier station. The colluvium groundwater contribution is correlated negatively with PDD at the Ratier station. In contrast, the fractured gneiss contribution showed no significant relation with PDD at the Ratier station. The fractured gneiss groundwater storage seem to be significant upstream of the catchment, but limited in comparison with the perennial input of the colluvium groundwater downstream. The saprolite water contribution is higher with high PDD at both sites. This confirms the assumptions made in the perceptual model, expecting higher groundwater contribution at low flow and higher saprolite water contribution at high flow. It also confirms a significant contribution of the colluvium aquifer at the Ratier station.

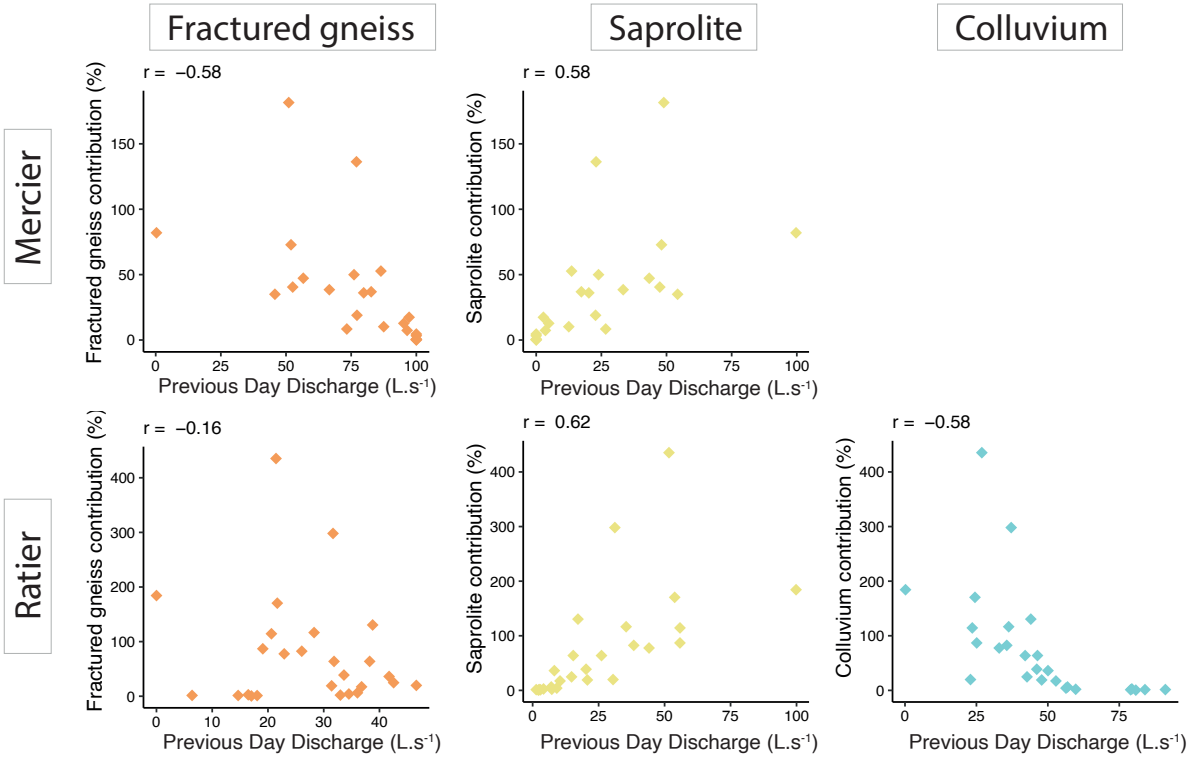

Figure 8 – Relation between the estimated contribution of runoff-generating sources and Previous Day Discharge at the Mercier and Ratier stations.

4 Discussion

4.1 Reliability of runoff-generating sources geochemical signatures

Even though the dataset we used included simple geochemical parameters, it allowed for the definition of precise source signatures significantly represented by tracers Li, Zn and Al. Other tracer combination were tested with mixing diagrams but none of them showed streamwater samples included in the end-member general shape (e.g., Rb-HCO_3^--Cr, see Figure S1S).

We found Li to be an almost exclusive tracer of the colluvium aquifer. The high Li concentrations observed at low flow for the Ratier station (median 13.6 µg/L) remain in the concentration range observed in natural stream water (Bingham et al., 1964). Concentrations of Li in natural waters depend on geological, topographical and hydrogeological conditions (Kavanagh et al., 2017). Dissolved Li can reach 1 to 20 µg/L in freshwater (Bingham et al., 1964). The main origin of natural Li is dissolution from siliceous matrix and some clayous minerals (Taylor, 1964). According to the geological information available, the colluvium formation is composed of a mix of clayous sands, basement rocks fragments (granite, gneiss...), siliceous pebbles and clayous-ferruginous matrix. This variety of geological origins could explain the presence of Li-bearing minerals. An anthropogenic origin of Li was also considered due to the presence of several potential pollution sources in the colluvium area. The BASIAS (Inventory of Abandoned Industrial Sites) and BASOL (Inventory of the contaminated sites) French databases showed at least three former industries located on top of the colluvium formation. However, as no previous or present effluent to stream river has been reported for these industries, the natural origin of Li is preferred.

The similarities in geochemical signatures between the fractured gneiss and colluvium groundwater forced the selection of a specific geochemical parameter of the fractured gneiss groundwater. We showed that the tracers of fractured gneiss groundwater were B, Zn, Co, K^+ and Rb. However, Co and K^+ did not show significant lower concentrations for high PDD samples compared to other samples. Parameters B and Zn were measured at higher concentrations than Rb at the Mercier station, making these parameters more reliable tracers. However, concentration of B may easily be enriched via wastewaters, and the presence of sewer overflow devices in the studied catchment does not favour the use of B as a tracer of fractured gneiss groundwater. The use of Zn is questionable, as this element is usually known to be marker of industrial or agricultural pollutions to soils and streamwater (El Azzi et al., 2016; Neal et al., 1996). No main anthropogenic sources of Zn, such as wastewater treatment plants, metallurgic or steel industry, have been reported in the area. An overview of the local satellite images from the Quickbird satellite shows the absence of any zinc roofs or major roads that could lead to significant zinc loads with urban surface runoff (Jacqueminet et al., 2013). Zn can also have lithological origins in some sedimentary formation or in presence of sulphide minerals such as galena or sphalerite (Fröhlich et al., 2008; Neal et al., 1996). Investigations conducted in 1980 by the French Geological Survey (BRGM) at 1 km south of the Mercier station showed the presence of significant amounts of Zn, up to 1000 mg/kg in some veins within the fractured gneiss (Carroue et Paquier, 1980). Thus, Zn can be considered as a good representative

tracer of the fractured gneiss groundwater.

Aluminium was chosen as the tracer of the saprolite water flow, among parameters Cr, DOC, Ni, NO_3^-, Cu and Ti. Aluminium can be released from alumina-silicates, which can be found in clayous minerals within saprolite formations, especially from granitic and gneissic bedrocks (Butt, 1983). It has low solubility in water leading to high concentrations in the particulate phase and low concentrations in the dissolved phase, which could explain why it is not usually used in mixing models. Some studies do consider it as a potential tracer of sources (e.g., Barthold et al., 2011), albeit showing complex interactions with hydrological mixing and biogeochemical processes (Wu et al., 2022). Results showed that Al concentrations correlated very well with PDD ($r = 0.822$).

According to our perceptual model, high PDD conditions may bring a major contribution of saprolite water flow. Yet, due to its non-conservative characteristics, no previous studies used Al as a representative tracer in an mixing model. In our study, estimating runoff-generating contributions at the scale of the Ratier catchment could allow the use of this non-conservative geochemical parameter, as no major interactions have time to occur between the release of Al from soil and the stream outlet. Indeed, the travel time in this relatively small catchment is estimated around 1 to 2 h for soil water.

The complete EMMA approach would have consisted to apply a Principal Component Analysis (PCA) with Li, Zn and Al selected concentrations, and use projected coordinates to resolve the mixing model equations. As only three end-members were considered in our study with fixed tracer concentrations, we preferred a simpler approach without applying PCA.

4.2 Evaluation of the hydrological perceptuel model

The framework from Wagener et al. (2007) was used as a template, modified according to our personal perception and knowledge, to build our perceptual model of the Ratier catchment. As we based the source identification on our perceptual model, we expected it to influence the results. We compared mean estimated contributions with other studies in similar geological contexts, and similar or different initial perceptual models. As we considered the sampling campaign to be representative of the global hydrological behaviour in non-rainy periods, we calculated the mean estimated contribution over the sampling period, from March 2017 to December 2019. We calculated mean contributions of 23% for fractured gneiss groundwater and 76% for saprolite subsurface water at the Mercier station. At the Ratier station, mean contributions are 21% for fractured gneiss groundwater, 61% for saprolite and 18% for colluvium groundwater. Soulsby et al. (2003) showed that groundwater from a granite aquifer in the Feugh catchment (Scotland), with limited storage, contributed to runoff no more than 30% over a year. In the same way, Hoeg et al. (2000) and Uhlenbrook et al. (2002) estimated a long-term contribution of groundwater around 20% for the Brugga and Zatler catchments in Germany, composed of gneiss bedrock covered by thin weathered soils. In these studies, they assigned the remaining contribution to saprolite water flow in the upper saprolite layer. A series of studies took place at the Panola Mountain research catchment in Georgia, U.S.A. (e.g., Aulenbach et al., 2021 ; Burns et al., 2001 ; Christophersen et Hooper, 1992 ; Hooper et al., 1990). The Panola Mountain catchment has crystalline formations with saprolite covering

bedrock up to 5 m width. Peters et Ratcliffe (1998) estimated a mean annual groundwater contribution of 75%. They assigned the remaining 25% to direct surface runoff during rain events, a contribution that was not considered in the present study. The perceptual model of Aulenbach et al. (2021) for the Panola catchment also considered a major contribution of the fractured gneiss groundwater to the stream (74% for a 1-year period). Our results are in strong opposition with Panola catchment estimations, albeit showing similar geological and hydrological context characteristics, but are consistent with results from the Feugh, Brugga and Zatler catchments. In their perceptual model, Peters et Ratcliffe (1998) and Aulenbach et al. (2021) suggested an unclear discrimination between the fractured bedrock groundwater and the saprolite water, whereas in our perceptual model of the Ratier catchment, we expected a clear distinction between these two runoff-generating sources. These differences show the influence of the initial perceptual model on the estimated contributions, making them hard to compare from a study to another.

4.3 Microbial parameters as markers of specific land cover in a mixed land-use catchment

Microbial DNA targets indicative of faecal matters were used in this study to differentiate the saprolite waters from the agricultural and urban areas of the catchments. These DNA targets are from bacteria unable to grow outside their host. Such targets can thus be used as tracers in a mixed land-use catchment. They can bring new knowledge on the impact of some activities on the long-term contamination of underground waters. In this study, the bacterial DNA target for ruminant contamination did not show major distribution biases between the Mercier and Ratier catchments. However, it is to be noted that these ruminant DNA signatures were found in both, the infiltrating waters of the saprolite and of the fractured gneiss. A human faecal contamination of the fractured gneiss waters was also highlighted by the detection of the HF183 DNA targets in these infiltrating waters.

Parameters like K^+, PO_4^{3-}, NH_4^+ or B were considered as tracers of wastewaters (Tjadraatmadja et Diaper, 2006). However, no significant positive correlation between the microbial parameters used in this study and these elements could be found. These geochemicals are highly reactive and not exclusive to wastewaters, which likely reduced the ability to recover them from the river waters over dry periods. It now remains to determine the time which can take for such a microbial tracer to spread from its source of emission down into the fractured gneiss infiltrated waters and the receiving stream. This will likely depend upon the thickness of the saprolite layer and complexity of the gneiss fractures including their size.

Two additional microbial DNA targets were investigated in this study : one targeting *P. aeruginosa* and one the clinical type 1 integron. Numbers of type 1 clinical integrons appeared to be in line with the overall distribution of the DNA targets indicative of human and ruminant faecal contaminations. The *P. aeruginosa* qPCR counts showed a more restricted distribution pattern. A higher prevalence was observed in the Mercier stream waters.

We expected the use of microbial DNA targets to help discriminate inputs to the saprolite flow in a mixed land-use catchment. However, these waters appeared significantly

contaminated by both agricultural and human faecal inputs. Human faecal contaminations appeared to significantly impact both streams despite the absence of a combined sewer overflow device in the Mercier catchment. A contamination from septic tanks located upstream the Mercier sampling station could explain these data.

5 Conclusions and perspectives

The objective of this study was to identify the runoff-generating sources and their contributions to the stream using an indirect method based on a simple biogeochemical dataset. The dataset used was built from monthly biogeochemical observations of major ions, carbonates, dissolved silica, dissolved organic carbon, trace elements and microbial parameters. In the initial perceptual model of the Ratier catchment, we considered three main runoff-generating sources in non-rainy periods : the colluvium aquifer located downstream of the catchment, the fractured gneiss aquifer in the rest of the catchment, and the saprolite layer on top of the gneiss formation. We selected the geochemical parameters Zn, Li and Al as tracers to estimate each of the respective fractured gneiss, colluvium and saprolite contributions using a mixing model. Results showed seasonally variable contributions with higher fractured gneiss and colluvium inputs in summer, and higher saprolite water contribution in winter. The average estimated contributions were consistent with field observations, and literature, and confirmed our perceptual model. The use of microbial parameters showed a significant and homogeneous contamination by both agricultural and human faecal inputs through the Ratier mixed land-use catchment.

This study showed the significant interest of a simple monthly monitoring dataset to enhance understanding of water pathways in a mixed land-use catchment. Thousands of streams and rivers in the world are monitored at similar frequency, and numerous biogeochemical datasets remain to be exploited. The method we set up allows for the interpretation of such data to better understand a catchment hydrology for any of these monitored streams. We also showed that some geochemical parameters, not often used in literature as tracers, such as Zn and Al, can bring relevant information on the runoff-generating sources. However, it is important to take into account the catchment scale to evaluate the option of using non-conservative geochemical parameters as tracers of hydrological sources.

Evaluating contributions estimated from an indirect method and streamwater samples only is difficult, though. Direct source sampling could assess the biogeochemical signatures of runoff-generating sources. The colluvium groundwater signature could be confirmed by sampling the stream draining the colluvium aquifer east of the basin. Using isotopic data (e.g., Deuterium, Oxygen-18) may assess estimations on groundwater and saprolite contributions. Moreover, additional sources are expected in a mixed-land-use catchment, particularly at the event scale. Sampling surface runoff water from homogeneous elementary sub-basins could provide biogeochemical signatures of specific natural, agricultural or urban runoff-generating sources (McElmurry et al., 2014). This method could be applied at the event scale to estimate their specific contributions at an infra-hour temporal resolution. In this context, the use of microbial data should show a great potential in the identification of agricultural and human contamination to stream total runoff. Dissolved organic matter could also give additional information on inputs from specific land covers to stream water (Boukra et al., 2023 ; Pernet-Coudrier et al., 2011). Such method could finally help validating the water pathways and flux calculated by conceptual and/or a physically based hydrological models.

Références

Appelo, C. A. J., & Postma, D. (2004). *Geochemistry, groundwater and pollution*. CRC press.

Argent, R. M., Western, A. W., & Neumann, L. E. Hydrological process investigation using water quality monitoring data. In : In *Proceedings ofthe International Congress on Modelling and Simulation*. 2007, 2347-2353.

Aulenbach, B. T., Hooper, R. P., van Meerveld, H. J., Burns, D. A., Freer, J. E., Shanley, J. B., Huntington, T. G., McDonnell, J., & Peters, N. E. (2021). The evolving perceptual model of streamflow generation at the Panola Mountain Research Watershed. *Hydrological Processes*, *35*(4).

Barthold, F. K., Tyralla, C., Schneider, K., Vaché, K. B., Frede, H.-G., & Breuer, L. (2011). How many tracers do we need for end member mixing analysis (EMMA) ? A sensitivity analysis. *Water Resources Research*, *47*(8).

Beven, K. (1991). Spatially Distributed Modeling : Conceptual Approach to Runoff Prediction. In D. S. Bowles & P. E. O'Connell (Éd.), *Recent Advances in the Modeling of Hydrologic Systems* (p. 373-387). Springer Netherlands.

Beven, K. (2012). *Rainfall-Runoff Modelling : the Primer, Second Edition* (T. 457). John Wiley & Sons, Ltd.

Bingham, F. T., Bradford, G. R., & Page, A. L. (1964). Toxicity of lithium to plants. *Calif Agr*, *18*(9), 6-7.

Birkel, C., & Soulsby, C. (2015). Advancing tracer-aided rainfall-runoff modelling : A review of progress, problems and unrealised potential. *Hydrological Processes*, *29*(25), 5227-5240.

Bouchali, R., Mandon, C., Marti, R., Michalon, J., Aigle, A., Marjolet, L., Vareilles, S., Kouyi, G. L., Polomé, P., Toussaint, J.-Y., & Cournoyer, B. (2022). Bacterial assemblages of urban microbiomes mobilized by runoff waters match land use typologies and harbor core species involved in pollutant degradation and opportunistic human infections. *Science of The Total Environment*, *815*, 152662.

Boukra, A., Masson, M., Brosse, C., Sourzac, M., Parlanti, E., & Miège, C. (2023). Sampling terrigenous diffuse sources in watercourse : Influence of land use and hydrological conditions on dissolved organic matter characteristics. *Science of The Total Environment*, *872*, 162104.

Branger, F., Kermadi, S., Jacqueminet, C., Michel, K., Labbas, M., Krause, P., Kralisch, S., & Braud, I. (2013). Assessment of the influence of land use data on the water balance components of a peri-urban catchment using a distributed modelling approach. *Journal of Hydrology*, *505*, 312-325.

Braud, I., Branger, F., Chancibault, K., Jacqueminet, C., Breil, P., Chocat, B., Debionne, S., Dodane, C., Honegger, A., Joliveau, T., Kermadi, S., Leblois, E., Lipeme Kouyi, G., Michel, K., Mosini, M., Renard, F., Rodriguez, F., Sarrazin, B., Schmitt, L., ... Viallet, P. (2011). *Assessing the Vulnerability of PeriUrban Rivers. Rapport scientifique final du projet AVuPUR (ANR-07-VULN-01)*. IRSTEA.

Burns, D., McDonnell, J., Hooper, R., Peters, N., Freer, J., Kendall, C., & Beven, K. (2001). Quantifying contributions to storm runoff through end-member mixing analysis and hydrologic measurements at the Panola Mountain research watershed (Georgia, USA). *Hydrological Processes*, *15*(10), 1903-1924.

Butt, C. R. M. (1983). Aluminosilicate cementation of saprolites, grits and silcretes in Western Australia. *Journal of the Geological Society of Australia*, *30*(1-2), 179-186.

Carroue, J., & Paquier, J. (1980). *Prospection sur la structure à barytine, fluorine et galène de Vaugneray*. BRGM.

Christophersen, N., & Hooper, R. (1992). Multivariate analysis of stream water chemical data : The use of principal components analysis for the end-member mixing problem. *Water Resources Research*, *28*(1), 99-107.

Colinon, C., Deredjian, A., Hien, E., Brothier, E., Bouziri, L., Cournoyer, B., Hartman, A., Henry, S., Jolivet, C., Ranjard, L., & Nazaret, S. (2013). Detection and enumeration of Pseudomonas aeruginosa in soil and manure assessed by an ecfX qPCR assay. *Journal of Applied Microbiology*, *114*(6), 1734-1749.

David, L., Elmi, S., & Féraud, J. (1979). Carte géologique de la France au 1/50 000 - Lyon. Feuille XXX-31. *BRGM, Service Géologique National*, 41.

Delfour, J., Dufour, E., Feybesse, J. I., Johan, V., Kerrien, Y., Lardeaux, J. M., Lemière, B., Mouterde, R., & Tegyey, M. (1989). Notice explicative, Carte géol. France (1/50000), feuille Tarare (697). *Orléans : Bureau de recherches géologiques et minières*, 120.

Deverel, S., Goldberg, S., & Fujii, R. (2011). Chemistry of Trace Elements in Soils and Groundwater.

El Azzi, D., Probst, J. L., Teisserenc, R., Merlina, G., Baqué, D., Julien, F., Payre-Suc, V., & Guiresse, M. (2016). Trace element and pesticide dynamics during a flood event in the save agricultural watershed : soil-river transfer pathways and controlling factors. *Water, Air, and Soil Pollution*, *227*(12).

Fenicia, F., Kavetski, D., Savenije, H. H. G., Clark, M. P., Schoups, G., Pfister, L., & Freer, J. (2014). Catchment properties, function, and conceptual model representation : Is there a correspondence ? *Hydrological Processes*, *28*(4), 2451-2467.

Fenicia, F., & McDonnell, J. J. (2022). Modeling streamflow variability at the regional scale : (1) perceptual model development through signature analysis. *Journal of Hydrology*, *605*, 127287.

Fröhlich, H., Breuer, L., Frede, H.-G., Huisman, J., & Vaché, K. (2008). Water source characterization through spatiotemporal patterns of major, minor and trace element stream concentrations in a complex, mesoscale German catchment. *Hydrological Processes*, *22*(12), 2028-2043.

Gassama Sow, A., Aïdara-Kane, A., Barraud, O., Gatet, M., Denis, F., & Ploy, M. C. (2010). High prevalence of trimethoprim-resistance cassettes in class 1 and 2 integrons in Senegalese Shigella spp isolates. *J Infect Dev Ctries*, *4*(04), 207-212.

Giri, S., & Qiu, Z. (2016). Understanding the relationship of land uses and water quality in Twenty First Century : A review. *Journal of Environmental Management*, *173*, 41-48.

Gnann, S. J., McMillan, H., Woods, R. A., & Howden, N. J. K. (2021). Including Regional Knowledge Improves Baseflow Signature Predictions in Large Sample Hydrology. *Water Resources Research*, *57*(2).

Goutaland, D. (2009). *Programme ANR AVuPUR - Prospection géophysique par panneau éléctrique de trois parcelles d'un sous-bassin versant de l'Yzeron*. CETE de Lyon.

Haag, I., & Westrich, B. (2002). Processes Governing River Water Quality Identified by Principal Component Analysis. *Hydrological Processes*, *16*, 3113-3130.

Hoeg, S., Uhlenbrook, S., & Leibundgut, C. (2000). Hydrograph separation in a mountainous catchment - combining hydrochemical and isotopic tracers. *Hydrological Processes*, *14*(7), 1199-1216.

Hooper, R. P., Christophersen, N., & Peters, N. E. (1990). Modelling streamwater chemistry as a mixture of soilwater end-members - An application to the Panola Mountain catchment, Georgia, U.S.A. *Journal of Hydrology*, *116*(1-4), 321-343.

Hrachowitz, M., Soulsby, C., Tetzlaff, D., Dawson, J. J. C., Dunn, S. M., & Malcolm, I. A. (2009). Using long-term data sets to understand transit times in contrasting headwater catchments. *Journal of Hydrology*, *367*(3-4), 237-248.

Jacqueminet, C., Kermadi, S., Michel, K., Béal, D., Gagnage, M., Branger, F., Jankowfsky, S., & Braud, I. (2013). Land cover mapping using aerial and VHR satellite images for distributed hydrological modelling of periurban catchments : Application to the Yzeron catchment (Lyon, France). *Journal of Hydrology*, *485*, 68-83.

Jankowfsky, S., Branger, F., Braud, I., Gironás, J., & Rodriguez, F. (2013). Comparison of catchment and network delineation approaches in complex suburban environments : application to the Chaudanne catchment, France. *Hydrological Processes*, *27*(25), 3747-3761.

Kavanagh, L., Keohane, J., Cleary, J., Garcia Cabellos, G., & Lloyd, A. (2017). Lithium in the Natural Waters of the South East of Ireland. *International Journal of Environmental Research and Public Health*, *14*(6).

Kendall, C., McDonnell, J., & Gu, W. (2001). A look inside 'black box' hydrograph separation models : A study at the hydrohill catchment. *Hydrological Processes*, *15*(10), 1877-1902.

Klaus, J., & McDonnell, J. (2013). Hydrograph Separation Using Stable Isotopes : Review and Evaluation. *Journal of Hydrology*, *505*, 47-64.

Knapp, J. L. A., von Freyberg, J., Studer, B., Kiewiet, L., & Kirchner, J. W. (2020). Concentration–discharge relationships vary among hydrological events, reflecting differences in event characteristics. *Hydrology and Earth System Sciences*, *24*(5), 2561-2576.

Ladouche, B., Probst, A., Viville, D., Idir, S., Baqué, D., Loubet, M., Probst, J.-L., & Bariac, T. (2001). Hydrograph separation using isotopic, chemical and hydrological approaches (Strengbach catchment, France). *Journal of Hydrology*, *242*(3-4), 255-274.

Lafont, M., Vivier, A., Nogueira, S., Namour, P., & Breil, P. (2006). Surface and Hyporheic Oligochaete Assemblages in a French Suburban Stream. *Hydrobiologia*, *564*(1), 183-193.

Lagouy, M., Branger, F., Thollet, F., Breil, P., & Dramais, G. (2015). *Suivi hydrologique du bassin versant périurbain de l'Yzeron*. Irstea.

Lamprea, K., & Ruban, V. (2011). Pollutant concentrations and fluxes in both stormwater and wastewater at the outlet of two urban watersheds in Nantes (France). *Urban Water Journal*, *8*(4), 219-231.

Le Moigne, P., Besson, F., Martin, E., Boé, J., Boone, A., Decharme, B., Etchevers, P., Faroux, S., Habets, F., Lafaysse, M., Leroux, D., & Rousset-Regimbeau, F. (2020). The latest improvements with SURFEX v8.0 of the Safran–Isba–Modcou hydrometeorological model for France. *Geoscientific Model Development*, *13*(9), 3925-3946.

Lepot, B., & Marescaux, N. (2022). *Opérations d'échantillonnage d'eau en cours d'eau dans le cadre des programmes de surveillance DCE - Recommandations techniques*. AQUAREF.

Marti, R., Ribun, S., Aubin, J.-B., Colinon, C., Petit, S., Marjolet, L., Gourmelon, M., Schmitt, L., Breil, P., Cottet, M., & Cournoyer, B. (2017). Human-driven microbiological contamination of benthic and hyporheic sediments of an intermittent peri-urban river assessed from MST and 16S rRNA genetic structure analyses. *Frontiers in Microbiology*, *8*, 19.

McDonnell, J. (1990). A Rationale for Old Water Discharge Through Macropores in a Steep, Humid Catchment. *Water Resources Research*, *26*(11), 2821-2832.

McElmurry, S. P., Long, D. T., & Voice, T. C. (2014). Stormwater dissolved organic matter : Influence of land cover and environmental factors. *Environmental Science and Technology*, *48*(1), 45-53.

McGlynn, B. L., McDonnel, J. J., & Brammer, D. D. (2002). A review of the evolving perceptual model of hillslope flowpaths at the Maimai catchments, New Zealand. *Journal of Hydrology*, *257*(1-4), 1-26.

McMillan, H., Clark, M., Woods, R., Duncan, M., Srinivasan, M. S., Western, A., & Goodrich, D. Improving perceptual and conceptual hydrological models using data from small basins. In : *336*. 2010, 264-269.

McMillan, H., Clark, M. P., Bowden, W. B., Duncan, M., & Woods, R. A. (2011). Hydrological field data from a modeller's perspective : Part 1. Diagnostic tests for model structure. *Hydrological Processes*, *25*, 511-522.

Mejía, A. I., & Moglen, G. E. (2010). Spatial distribution of imperviousness and the space-time variability of rainfall, runoff generation, and routing. *Water Resources Research*, *46*(7).

Météo-France. (2023). [Online] Available in : https ://meteofrance.com/climat/normales/france/auvergn rhone-alpes/LYON-BRON.

Mosley, M. P. (1979). Streamflow generation in a forested watershed, New Zealand. *Water Resources Research*, *15*(4), 795-806.

Mullen, K. M., & van Stokkum, I. H. M. (2012). *nnls : The Lawson-Hanson algorithm for non-negative least squares (NNLS).*

Navratil, O., Boukerb, M. A., Perret, F., Breil, P., Caurel, C., Schmitt, L., Lejot, J., Petit, S., Marjolet, L., & Cournoyer, B. (2020). Responses of streambed bacterial groups to cycles of low-flow and erosive floods in a small peri-urban stream. *Ecohydrology*, *13*(4), e2206.

Neal, C., Smith, C., Jeffery, H., Jarvie, H., & Robson, A. (1996). Trace element concentrations in the major rivers entering the Humber estuary, NE England. *Journal of Hydrology*, *182*(1-4), 37-64.

Paulet, J.-P. (2009). *Manuel de géographie urbaine.* Armand Colin.

Pearce, A., Stewart, M., & Sklash, M. (1986). Storm Runoff Generation in Humid Headwater Catchments : 1. Where Does the Water Come From ? *Water Resources Research*, *22*(8), 1263-1272.

Pernet-Coudrier, B., Varrault, G., Saad, M., Croue, J. P., Dignac, M.-F., & Mouchel, J.-M. (2011). Characterisation of dissolved organic matter in Parisian urban aquatic systems : predominance of hydrophilic and proteinaceous structures. *Biogeochemistry*, *106*(1), 89-106.

Peters, N., & Ratcliffe, E. (1998). Tracing Hydrologic Pathways Using Chloride at the Panola Mountain Research Watershed, Georgia, USA. *Water Air and Soil Pollution*, *105*, 263-275.

Peters, N. E., Freer, J., & Aulenbach, B. T. (2003). Hydrological Dynamics of the Panola Mountain Research Watershed, Georgia. *Groundwater*, *41*(7), 973-988.

Pinder, G. F., & Jones, J. F. (1969). Determination of the ground-water component of peak discharge from the chemistry of total runoff. *Water Resources Research*, *5*(2), 438-445.

Pozzi, A. C., Petit, S., Marjolet, L., Youenou, B., Lagouy, M., Namour, P., Schmitt, L., Navratil, O., Breil, P., Branger, F., & Cournoyer, B. (2024). Ecological assessment of combined sewer overflow management practices through the analysis of benthic and hyporheic sediment bacterial assemblages from an intermittent stream. *Science of The Total Environment*, *907*, 167854.

R Core Team. (2020). *R : A Language and Environment for Statistical Computing.* R Foundation for Statistical Computing. Vienna, Austria.

Soulsby, C., Rodgers, P., Smart, R., Dawson, J., & Dunn, S. (2003). A tracer-based assessment of hydrological pathways at different spatial scales in a mesoscale Scottish catchment. *Hydrological Processes*, *17*(4), 759-777.

Taylor, S. (1964). Abundance of chemical elements in the continental crust : a new table. *Geochimica et Cosmochimica Acta*, *28*(8), 1273-1285.

Tetzlaff, D., Malcolm, I., & Soulsby, C. (2007). Influence of forestry, environmental change and climatic variability on the hydrology, hydrochemistry and residence times of upland catchments. *Journal of Hydrology*, *346*(3), 93-111.

Thorndike, R. L. (1953). Who belongs in the family ? *Psychometrika*, *18*(4), 267-276.

Tjadraatmadja, G., & Diaper, C. (2006). *Sources of critical contaminants in domestic wastewater –a literature review*. CSIRO : Water for a Healthy Country National Research Flagship.

Tran, N. H., Reinhard, M., Khan, E., Chen, H., Nguyen, V. T., Li, Y., Goh, S. G., Nguyen, Q. B., Saeidi, N., & Gin, K. Y.-H. (2019). Emerging contaminants in wastewater, stormwater runoff, and surface water : Application as chemical markers for diffuse sources. *Science of The Total Environment*, *676*, 252-267.

Uhlenbrook, S., Frey, M., Leibundgut, C., & Maloszewski, P. (2002). Hydrograph separations in a mesoscale mountainous basin at event and seasonal timescales. *Water Resources Research*, *38*(6), 31-1-31-14.

United Nations. (2019). *World Urbanization Prospects : The 2018 Revision (ST/ESA/SER.A/420)*.

Vaissie, P., Monge, A., & Husson, F. (2021). *Factoshiny : Perform Factorial Analysis from 'FactoMineR' with a Shiny Application*.

Wagener, T., Sivapalan, M., Troch, P., & Woods, R. (2007). Catchment Classification and Hydrologic Similarity. *Geography Compass*, *1*(4), 901-931.

Walsh, C. J., Roy, A. H., Feminella, J. W., Cottingham, P. D., Groffman, P. M., & Morgan, R. P. (2005). The urban stream syndrome : current knowledge and the search for a cure. *Journal of the North American Benthological Society*, *24*(3), 706-723.

Wilson, C., & Weng, Q. (2010). Assessing Surface Water Quality and Its Relation with Urban Land Cover Changes in the Lake Calumet Area, Greater Chicago. *Environmental Management*, *45*(5), 1096-1111.

Wu, S., Tetzlaff, D., Goldhammer, T., Freymueller, J., & Soulsby, C. (2022). Tracer-aided identification of hydrological and biogeochemical controls on in-stream water quality in a riparian wetland. *Water Research*, *222*, 118860.

Supplementary material

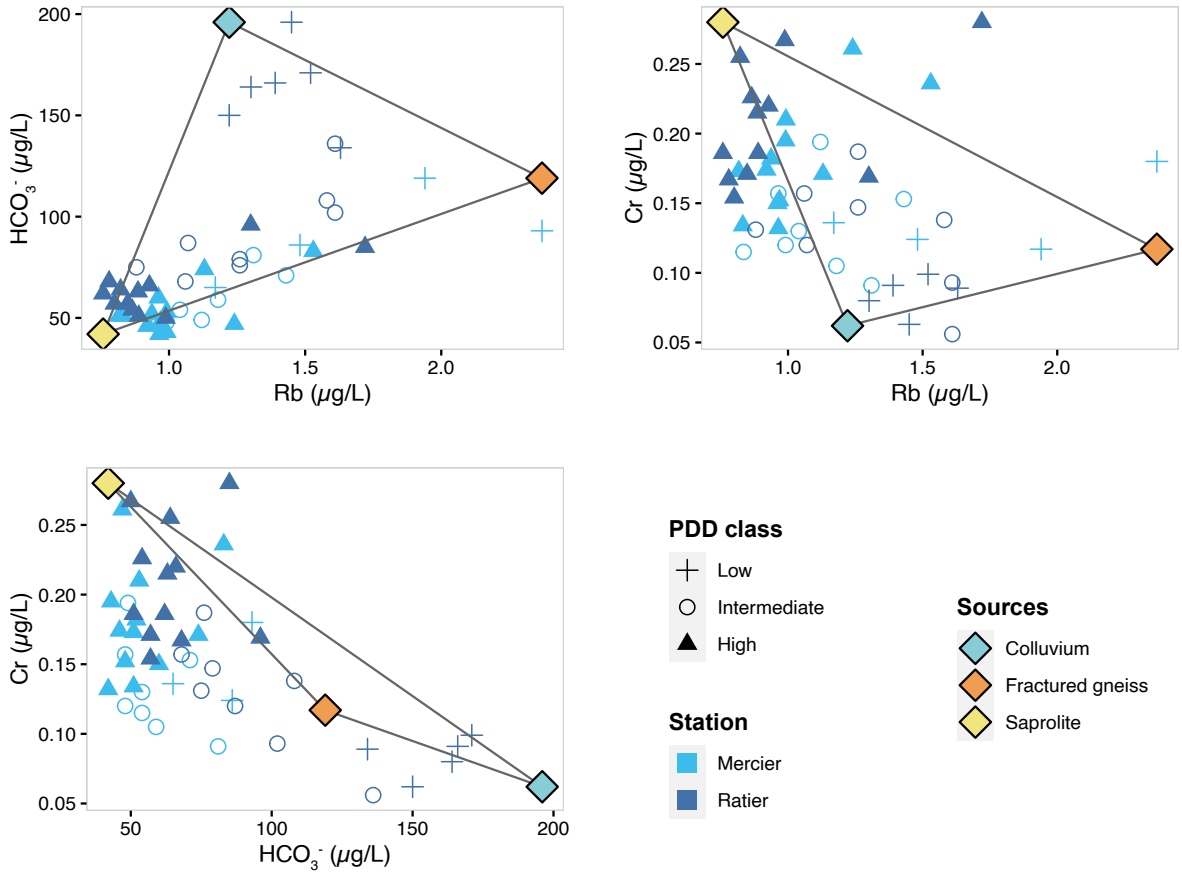

Figure S1 – Mixing diagrams showing samples and end-members concentrations of Rb, HCO_3^- and Cr at the Mercier and Ratier stations. PDD : Previous Day Discharge

Table S1 – Median and concentration range of major chemical parameters and trace elements at the Mercier and Ratier stations (number of surface water samples, n = 24 and 26 respectively ; collected from May 2017 to December 2018

Chemical parameter	Unit	Limit of quantification	Mercier		Ratier	
			Median	Range	Median	Range
Ca^{2+}	mg L^{-1}	4	25.0	14.0 - 45.1	35.4	19.4 - 66.9
Cl^-	mg L^{-1}	1	38.0	23.6 – 101.0	36.2	21.7 - 67.7
DOC	mg L^{-1}	0.2	6.8	5.3 – 10.0	6.4	2.8 - 10.2
HCO_3^-	mg L^{-1}	10	54	42 - 119	78	50 - 196
K^+	mg L^{-1}	1	3.3	1.4 - 4.7	3.5	2.3 - 4.4
Mg^{2+}	mg L^{-1}	1	4.1	2.9 - 6.2	5.2	3.2 – 9.0
Na^+	mg L^{-1}	1	22.0	16.4 - 50.8	22.3	16.2 - 33.1
NO_3^-	mg L^{-1}	1	5.5	1.0 - 24.2	7.1	3.3 – 27.0
PO_4^{3-}	mg L^{-1}	0.10	0.12	0.07-0.52	0.15	0.10-1.72
SO_4^{2-}	mg L^{-1}	1	17.9	12.5 - 50.2	27.6	15.3 - 80.4
SiO_2	mg L^{-1}	0.4	12.9	8.4 - 20.2	14.0	8.4 - 29.5
Al	µg L^{-1}	2	21.9	4.3 - 75.3	17.3	6.4 - 81.8
As	µg L^{-1}	0.005	1.01	0.770 - 2.92	1.52	1.10 - 3.60
B	µg L^{-1}	0.2	13.8	7.8 - 39.1	19.1	10.4 - 46.2
Ba	µg L^{-1}	0.02	20.1	11.3 - 32.4	29.5	16.1 - 48.1
Cd	µg L^{-1}	0.010	0.010	0.010 - 0.010	0.010	0.010 – 0.012
Co	µg L^{-1}	0.005	0.19	0.12 - 1.35	0.21	0.07 - 0.29
Cr	µg L^{-1}	0.02	0.15	0.09 - 0.26	0.16	0.06 - 0.28
Cu	µg L^{-1}	0.1	2.28	0.65 – 5.00	2.16	1.07 - 4.31
Fe	µg L^{-1}	0.1	55.8	18.5 - 446	54.0	22.6 - 165
Li	µg L^{-1}	0.01	0.68	0.50 - 1.56	1.29	0.68 - 20.6
Mn	µg L^{-1}	0.02	7.39	2.04 - 514	16.3	4.26 - 75.1
Mo	µg L^{-1}	0.01	0.17	0.12 - 0.36	0.32	0.16 - 1.42
Ni	µg L^{-1}	0.02	0.86	0.65 - 1.45	0.86	0.26 - 1.29
Pb	µg L^{-1}	0.005	0.09	0.04 - 0.29	0.10	0.01 - 0.53
Rb	µg L^{-1}	0.005	1.02	0.82 - 2.37	1.15	0.76 - 1.72
Sr	µg L^{-1}	0.01	91.8	54.2 - 137	121	67.6 - 210
Ti	µg L^{-1}	0.05	1.49	0.27 - 2.95	1.81	0.26 - 3.75
U	µg L^{-1}	0.05	0.15	0.09 - 0.41	0.35	0.21 - 1.61
V	µg L^{-1}	0.05	0.43	0.24 - 1.07	0.57	0.39 - 1.22
Zn	µg L^{-1}	0.1	1.6	0.56 - 23.8	1.61	0.49 - 8.15

Table S2 – Concentrations of microbial parameters at the Mercier and Ratier stations, collected from May 2017 to December 2018

Date	**Sampling station**	**Microbial parameters (log10 copy number /100mL)**			
		Human-specific *Bacteroides* marker HF183	**Ruminant-specific *Bacteroides* marker rum-2-bac**	**Class 1 clinic integron**	***P. aeruginosa***
29/05/17	Mercier	LD	4.1	LD	LD
	Ratier	4.6	4.0	LD	LD
05/07/17	Mercier	LD	LD	LD	3.2
	Ratier	4.3	LD	4.2	LD
07/09/17	Mercier	LD	LD	LQ	3.3
	Ratier	LQ	LD	LD	LD
03/10/17	Mercier	LD	LD	2.8	3.5
	Ratier	LQ	LD	LD	3.0
14/12/17	Mercier	3.8	3.9	LQ	2.4
	Ratier	4.3	LD	LD	LQ
09/01/18	Mercier	LD	LD	LQ	3.3
	Ratier	5.9	4.2	LD	LD
06/02/18	Mercier	4.3	3.4	LD	5.2
	Ratier	4.2	3.4	LD	4.5
06/03/18	Mercier	4.1	3.3	LD	4.7
	Ratier	2.8	4.5	LD	4.6
05/04/18	Mercier	LD	3.6	LD	4.2
	Ratier	LD	3.7	LD	4.2
07/05/18	Mercier	LD	2.4	2.4	4.7
	Ratier	LD	3.6	LD	2.9
06/06/18	Mercier	4.4	3.5	4.4	4.6
	Ratier	5.3	3.0	LD	5.0
11/07/18	Mercier	LD	LD	LD	LD
	Ratier	LD	LD	LD	LD
08/11/18	Mercier	3.5	1.7	LD	4.5
	Ratier	4.0	LD	LD	2.5
05/12/18	Mercier	2.7	LD	LD	LD
	Ratier	3.7	3.1	2.4	2.4